Available online at www.sciencedirect.com

ScienceDirect

Procedia Materials Science 8 (2015) 914 – 923

Procedia Materials Science

www.elsevier.com/locate/procedia

International Congress of Science and Technology of Metallurgy and Materials, SAM - CONAMET 2013

Effect of Heat Input on AA5052 Friction Stir Welds Characteristics

Leonardo N. Tufaro[a], Iván Manzoni[b], Hernán G. Svoboda[c,d,]*

[a]*Instituto Nacional de Tecnología Industrial, Centro de Investigación y Desarrollo en Mecánica, Av. Gral Paz 5445, B1650KNA, San Martín, Buenos Aires, Argentina*

[b]*Instituto Sabato, UNSAM-CNEA, Av. Gral Paz 1499, B1650KNA, San Martín, Buenos Aires, Argentina*

[c]*Laboratorio de Materiales y Estructuras, Facultad de Ingeniería, INTECIN, Universidad de Buenos Aires, Av. Las Heras 2214, C1127AAR, Ciudad Autónoma de Buenos Aires, Argentina*

[d]*Consejo Nacional de Investigaciones Científicas y Técnicas (CONICET), Av. Rivadavia 1917, C1033AAJ, Ciudad Autónoma de Buenos Aires, Argentina*

Abstract

Friction Stir Welding (FSW) is a relatively novel solid state welding process that strong enhanced the welding of aluminum alloys for structural applications. In this process, the heat necessary for the required plastic flow of material is produced at the interfase tool-work piece, being affected by factors such as rotational speed, axial load and tool shoulder diameter, among others. The objective of this work was to study the effect of tool shoulder diameter on heat input during FSW of AA5052-H32 alloy and the resulting characteristics of the produced welded joints. Tools of 10, 12, 14 and 16 mm shoulder diameter were constructed and used to butt weld plates of 3 mm thick of AA5052-H32 aluminum alloy. Welds were made with 514 rpm of rotational speed and 98 mm/min of welding speed. Thermal cycles were acquired during welding using thermocouples. Macrostructural characterization and Vickers microhardness profiles were done on each welded sample. It was observed an increase in power with shoulder diameter, as well as a lower level of defects in the stirred zone, related with an improved plastic flow. Hardness also decreased with tool diameter, due to a higher thermal effect on the microstructure.

Selection and peer-review under responsibility of the scientific committee of SAM - CONAMET 2013

Keywords: Friction Stir Welding (FSW); Aluminum; Heat Input; Tool Shoulder

* Corresponding author. Tel.: +5411-4514-3009; fax: +5411-4514-3009
E-mail address: hsvobod@fi.uba.ar

Selection and peer-review under responsibility of the scientific committee of SAM - CONAMET 2013
doi:10.1016/j.mspro.2015.04.152

1. Introduction

Friction Stir Welding (FSW) is a relatively novel solid state welding process, which has proved to have great potential for different materials, particularly aluminum alloys. FSW is based on the plastic flow of material produced by a non-consumable rotating tool inserted into the joint to be welded. The heat necessary to produce the required plastic flow for the conformation of the joint is mainly produced at the interface tool-work piece, being affected by factors such as rotational speed, welding speed, axial load and tool shoulder diameter (D), among others.

Schmidt and Hattel (2008) developed an analytical model for the heat generation in FSW. The most important difference between this model and previous ones is that it considers the contact condition at this interface by a parameter called slip rate (δ), which varies from 0 to 1. If the slip rate is 0, the contact condition is sliding, and if it is 1, the contact condition is sticking. Moreover, although it has been reported that the heat input (HI) generated by the tool pin can become 20% of the total heat input, in this work the terms associated with the tool pin are omitted to simplify the analysis (Mishra and Ma, (2005); Mishra and Mahoney, (2007)). Therefore, based on that model, Equation 1 expresses power (Q) generated during FSW depending on the rotational speed (ω) and the tool shoulder diameter (D), considering that the shear yield stress (τ_y), the friction coefficient (μ), the contact pressure (p) and the slip rate (δ) are uniform throughout the interface.

$$Q = \frac{2}{3}\pi\left[\omega\left(\delta.\tau_y + (1-\delta)\mu.p\right)\right]\left(D/2\right)^3 \quad (1)$$

As shown in Equation 1, an increase of the D would produce a large increase in generated Q, if the remaining factors were kept constant. However, as many of the factors that appear in Equation 1 are temperature dependent, and this depends on the power, it is not easy to describe the effect of the increase of the D on the HI.

In the recent years, studies have been carried out about the influence of the tool shoulder diameter on the defect generation and mechanical properties of friction stir welds of AA6061 and AA 7075-T6 (Elangovan and Balasubramanian (2008); Rajakumar et al. (2011)). In these works, the increase of the D was only associated with an increase of HI, but it is not quantified nor explained the relationship between both factors. In this sense, more work is needed on this matter.

In FSW there are different types of defects related to the lack of HI, which generates an insufficient plastic flow. Therefore, the tunnel defect, the kissing bond and/or zigzag line, may be associated with lack of plastic flow and/or heat input (Mishra and Mahoney (2007); Oosterkamp et al. (2004)). In turn, the HI defines the volume of recrystallized material in the welding nugget (WN), the final grain size in this zone and metallurgical aspects as the microstructure degradation in the heat affected zone (HAZ) (Mishra and Ma (2005); Nandan et al. (2008)). Finally, the defect density and microstructural evolution, both associated with the thermal cycle during FSW, control the final properties of the joint (Mishra and Mahoney (2007)).

The objective of this work was to study the effect of D on HI during FSW of AA5052-H32 alloy and the characteristics of the joints obtained.

Nomenclature

δ	Slip Rate	TC	Thermocouple
D	Tool Shoulder Diameter	WN	Welding Nugget
FEM	Finite Element Method	WNA	Welding Nugget Area
FSW	Friction Stir Welding	τ_y	Shear Yield Stress
HAZ	Heat Affected Zone		
HI	Heat Input		
HV	Vickers Hardness		
P	Mean Pressure		
PT	Peak Temperature		
Q	Power		

2. Experimental procedure

In order to achieve the proposed objectives, plates of 150x75x3 mm of AA5052-H32 were butt welded by FSW using four tools with different shoulder diameters (10, 12, 14 and 16 mm). FSW tools were made of H13 tool steel and have of a concave shoulder with a smooth tapered pin with three machined flats at 120° to the axis of symmetry, as shown in Figure 1.a. For all cases, the pin length was 2.8 mm, with a base diameter of 3 mm. An image of the experimental set up used for FSW can be seen in Figure 1.b.

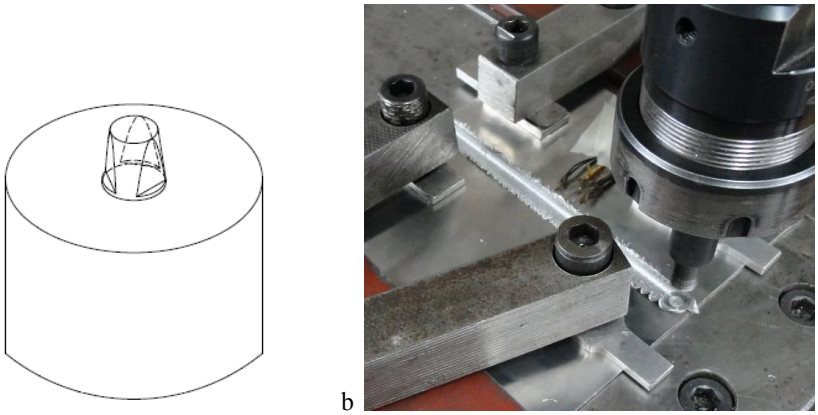

a b

Fig. 1. (a) Scheme of FSW tools; (b) FSW experimental set up.

During welding, thermal cycles were acquired using two K-type thermocouples. The thermocouples were positioned at 1 and 2 mm from the edge of the weld bead (TC1 and TC2, respectively) on the advancing side of the joint and near of the half length of the specimen, with a distance between them of 5 mm, as can be seen in Figure 1.b. The thermocouples were placed in machined holes of 1 mm in diameter and 1.5 mm in deep.

Table 1 shows the welding parameters used and the identification of the samples.

Table 1. FSW parameters

Identification	Shoulder Diameter (mm)	Rotational Speed (rpm)	Welding Speed (mm/min)	Tool Tilt Angle (º)
D10	10	514	98	1,5
D12	12			
D14	14			
D16	16			

Heat transfer during the welding process was modeled by finite elements method (FEM) to get the value of the net power (Q) from acquired thermal cycling. The heat transfer in the plates was considered two-dimensional, transient and considering only conduction. Furthermore, a spatial distribution of the heat source was used, proportional to the distance from the center of the source. Heat losses to the environment were taken into account, by conduction to the backing plate and convection in the remaining boundary surfaces. The final result was the net power (Q) necessary to obtain a calculated peak temperature in the position of TC1 equal to the peak temperature measured by the same thermocouple (Tufaro and Svoboda (2012)).

A strain gage attached in the head of the machine was used to measure axial load during welding, by means of a calibration curve strain-axial load, obtained previously (Fernandez (2009)). This strain is measured using a Strain Indicator P-3500, Vishay-Measurement Group.

From the welded samples cross sections were extracted from each specimen, which were prepared for macrographic observation and Vickers microhardness (HV) measurements. The different zones of the welded joints

and the presence of discontinuities associated with FSW were analyzed. Also, the welding nugget area was measured in each case. Microhardness profiles were obtained on the cross section along a line on the half thickness, with a load of 500 gf.

3. Results and discussion

3.1. Visual Inspection

Figure 2 shows the surface appearance of the welded samples obtained with different D.

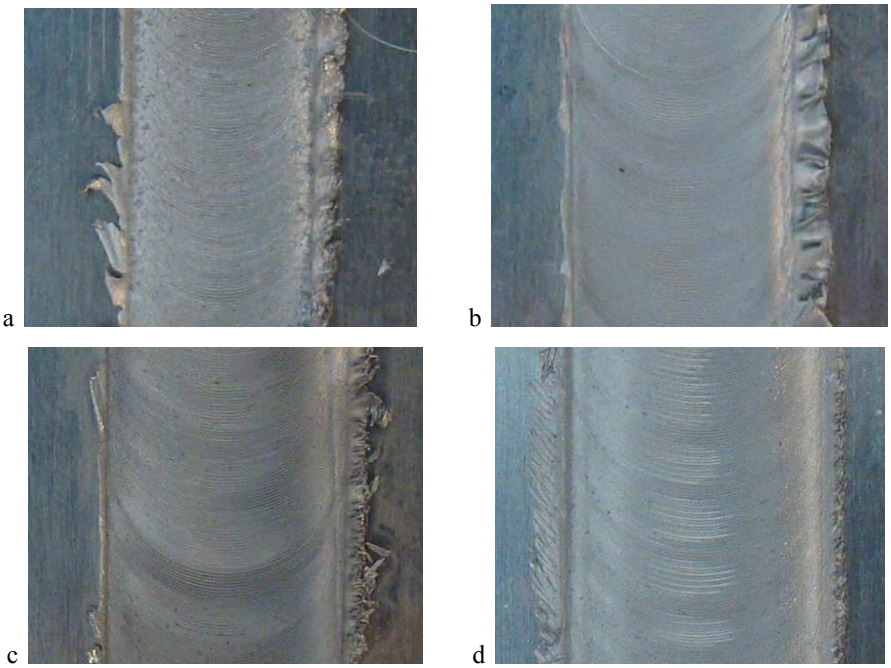

Fig. 2. Surface appearance of FSW welded samples with different D: (a) D10; (b) D12; (c) D14; (d) D16.

It can be seen that all of them had a satisfactory surface appearance, without the presence of detectable surface defects. It is also noted that the width of the weld bead was increased according to the used D.

3.2. Thermal cycles

As mentioned in the previous section, the thermocouples were located at 1 and 2 mm from the edge of the weld bead in each case. Thus, as it can be seen in Table 2, the distance between the TC and the joint centerline was different for each D. Also, it can be seen the peak temperature (PT) reached by TC1 and the calculated power (Q) from this measured PT, for each case.

Table 2. Thermocouples position and results from acquired thermal cycles

Designation	Distance between the TC and the Center Line (mm)		Peak Temperature for TC1 (ºC)	Power (W)
	TC1	TC2		
D10	6	7	273	372
D12	7	8	336	497
D14	8	9	333	513
D16	9	10	331	589

Figure 3 shows the thermal cycles acquired by both thermocouples for the four D studied. It can be seen that the peak temperature corresponding to the TC1 reach a maximum for D=12mm. Although the PT was expected to increase continuously with D, the trend obtained is a balance between a higher HI and a higher distance to the centerline, due to the change in the position of the TC. In turn, Q increased with the employed D.

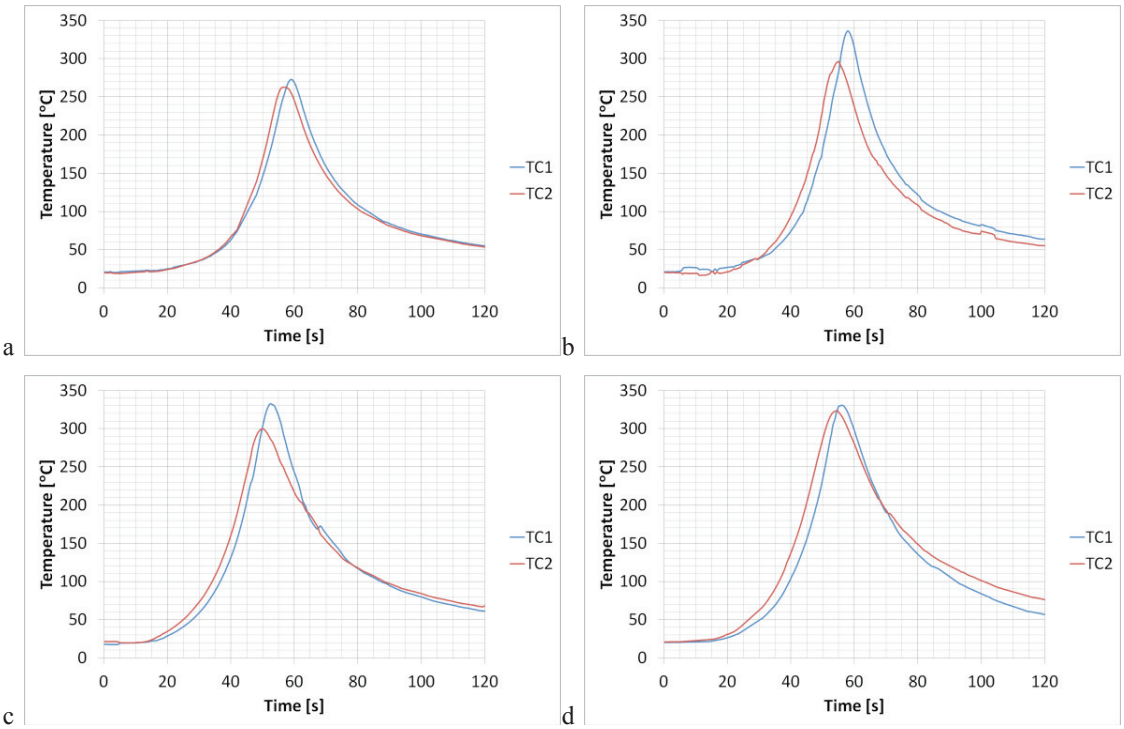

Fig. 3. Acquired thermal cycles of FSW welded specimens: (a) D10; (b) D12; (c) D14; (d) D16.

In Figure 4.a are plotted the peak temperatures profiles calculated by FEM for the different D such that the PT measured with TC1 (indicated in the figure with a filled blue marker) were equal to the calculated PT in the position of this TC. Thus, it can be clearly seen that if the TCs were positioned at the same distance from the centreline, PTs would be ever increasing. For example, this behavior can be observed by the dashed line plotted to 9 mm from the centreline in Figure 4.a. However, this is not convenient to perform in practice because for smaller shoulder diameters the TCs should be positioned away from the heat source, magnifying the error related with simplifying assumptions of the models (Tufaro and Svoboda, (2012)).

It can also be observed that as D increase, the calculated PT profiles become more uniform, which imply a smaller increase in calculated PTs. This behavior is related to the increased area covered by the heat source as D increases, resulting in a more uniform heat source density.

Moreover, in Figure 4.b are plotted the net power Q values calculated from the PTs corresponding to the TC1 from different D. It can be seen that Q increased linearly with D. An experimental expression was obtained to quantify this relationship, with a good degree of correlation.

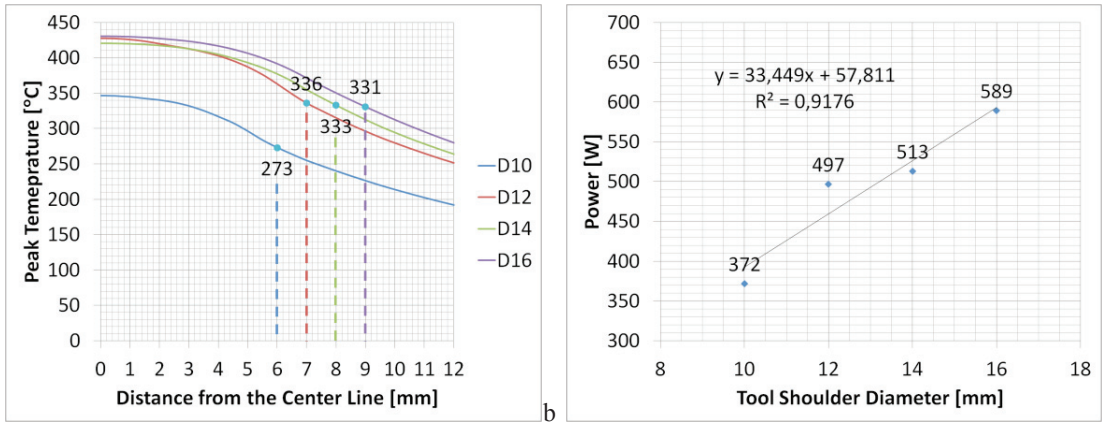

Fig. 4. Peak temperature profiles (a) and heat input (b) calculated by FEM from the peak temperature corresponding to the TC1 for different D

Analyzing the analytical model for heat generation in FSW expressed in Equation 1, Q increases with the cube of the D, if the remaining parameters are constant. Therefore, this set of parameters (δ, τ_y, μ, p) should decrease with increasing the shoulder diameter in such way that relationship between both parameters remains linear. For example, increasing D, increases Q and T, which implies a decrease in τ_y, associated with the heat generation for the sticking contact condition.

Finally, it should be clarified that the PT profile shown in Figure 4.a for the diameter D12 and the calculated Q exceeded the general trend (Figure 4.b), which could be related to the dispersion in the control of the set of variables associated with the measurements done.

3.3. Axial Load

Table 3 shows the results from the axial load measurement. In each case, the mean pressure was calculated as the ratio between the axial load and the projected area of the tool shoulder, corresponding to the area of a circle with a diameter equal to the shoulder diameter.

Table 3. Results from axial load measuring

Designation	Shoulder Diameter (mm)	Axial Load (kN)	Projected Area (mm^2)	Mean Pressure (MPa)
D10	10	4.7	79	60
D12	12	6.4	113	57
D14	14	7.4	154	48
D16	16	8.5	201	42

In Figure 5.a, the axial load values measured for each D are plotted. It can be seen that the axial load increased linearly with this parameter. Moreover, Figure 5.b shows the evolution of the mean pressure (P) with D. In this case, it is noted that the P decreased linearly with D. For both variables, experimental expressions were obtained to model the analyzed relationships, with a good degree of correlation.

These P values are representative of the contact pressure appearing in the analytical model for the heat generation in FSW presented in Equation 1. Thus, continuing the analysis of previous subsection, this decrease in contact pressure with the shoulder diameter implies a decrease of heat generation for the sliding contact condition.

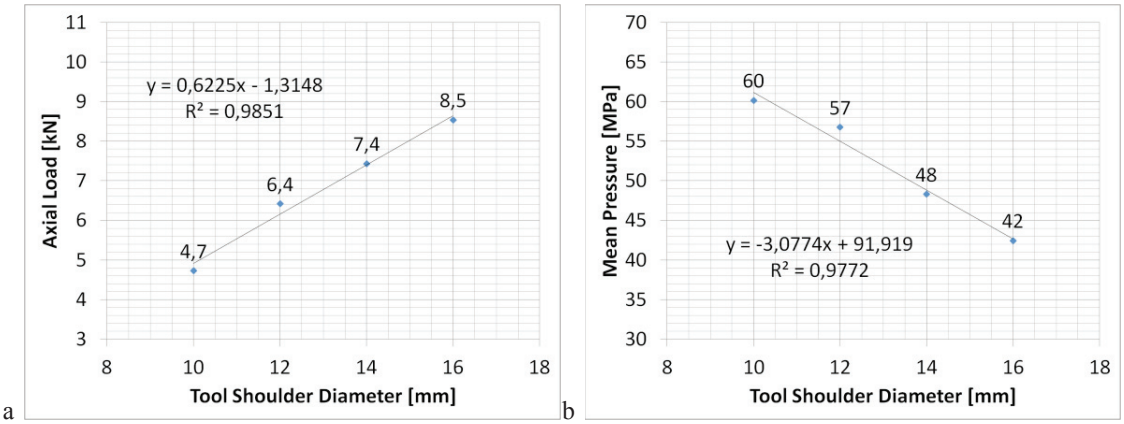

Fig. 5. Axial load (a) and mean pressure (b) vs. tool shoulder diameter.

Therefore, for both contact conditions, it may be explained why the power not increased with the cube of the shoulder diameter as it seems in the heat generation model of Equation 1. From these considerations emerge the need to take into account the temperature dependence of the other parameters (δ, τ_y, μ, p).

3.4. Macrostructural characterization

Figure 6 shows the macrographs of cross sections of the four FSW welded specimens, for different D.

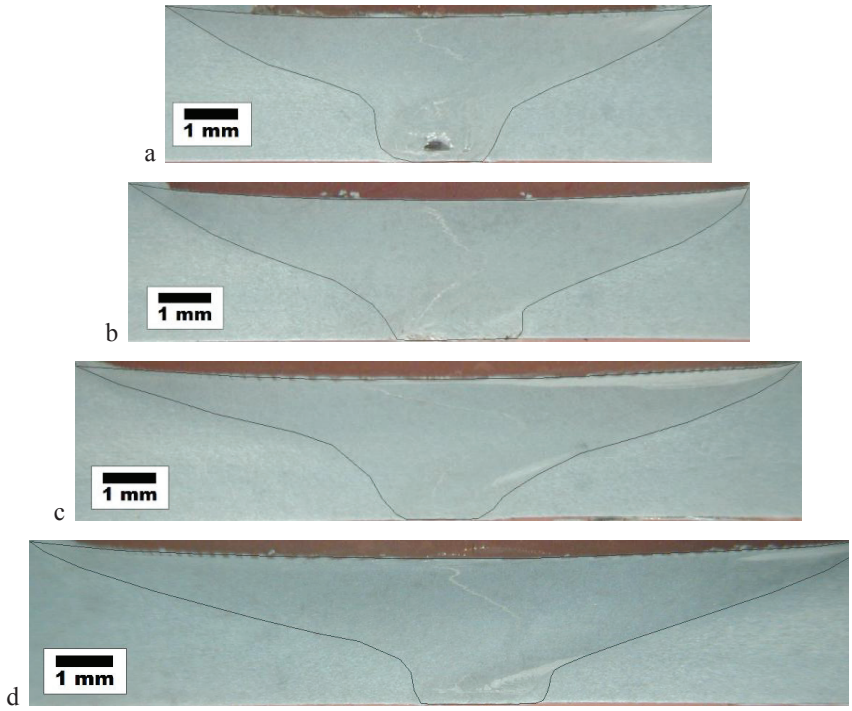

Fig. 6. Macrograph of FSW welded specimens: (a) D10; (b) D12; (c) D14; (d) D16.

It can be observed the different characteristics zones of FSW welded joints, showing full penetration in the root, in all cases. The advancing side is always located on the right side of the image. The black line that is shown in the

figure was used to calculate the welding nugget area. For D10 can be seen a tunnel defect related with the low HI introduced during the weld.

Although the WN shape was similar for all the welding conditions, it can be observed an increase in its size with D. For this reason, in Figure 7.a is analyzed the evolution of the welding nugget area (WNA) vs. D.

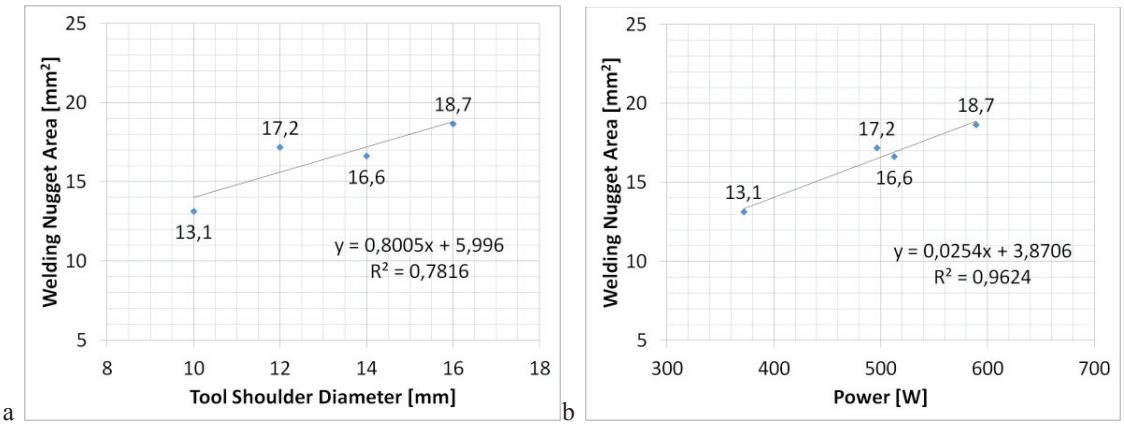

Fig. 7. Welding nugget area vs tool shoulder diameter (a) and power (b).

As it was observed with PTs profiles and calculated Q values, the WNA of the welded specimen D12 was found above of the general trend.

As it is known, an increase in Q involves an increase in temperature and in the plastic flow of material, so it is expected to obtain a better correlation between WNA and Q (Mishra and Ma, (2005)). Because of this, in Figure 7.b, WNA vs. Q is plotted, showing a linear trend with a better degree of correlation.

In macrographs of Figure 6 can be seen some discontinuities in the welding nugget of the specimen D10. Figure 8 shows a welding nugget detail of the four welding conditions.

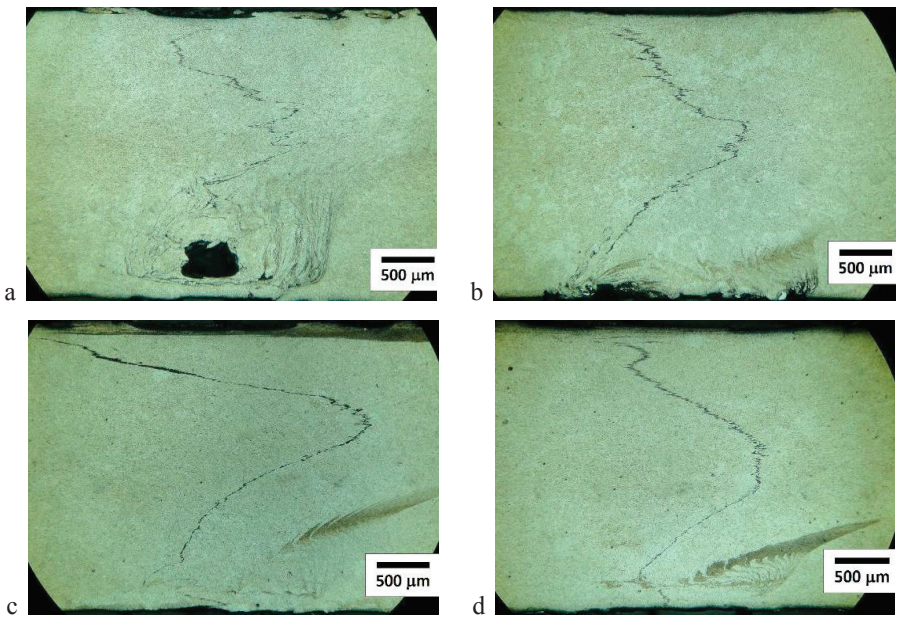

Fig. 8. Welding nugget detail of FSW welded specimens: (a) D10; (b) D12; (c) D14; (d) D16.

In the WN of the welded specimen D10, Figure 8.a, it can seen a defect near the root, which is generated due to lacking plastic flow of material, associated with a relatively low heat input. The material stirred by the tool should be able to fill the volume produced by the translation of the pin. If the generated heat is not sufficient, the deformed material is cooled before filling the region behind the tool, generating this type of defect (Mishra and Mahoney, (2007)).

Furthermore, is clearly observed a zigzag line in the WN of all welded specimens, which is another characteristic discontinuity of this process that can affect the mechanical properties of the joint, depending on its continuity. This zigzag line is the oxide layer remnant of the original surfaces to be joined. It is known that the separation and rupture of such layers depends on the plastic flow of material and heat input (Mishra and Mahoney, (2007)). However, it is observed in this figure that the variation of the shoulder diameter apparently do not have a great effect on the shape of this zigzag line.

Finally, besides the zigzag line corresponding to the oxide layers of the initial surfaces to be joined, other lines can be observed near the root in the WN of the welded specimen D10, Figure 8.a. These lines might be associated with the contact of the successive material layers deposited behind pin in each revolution of the tool.

The low HI limits the plastic flow and complicates the forging of the material for the formation of the metalurgical joint. In this way, oxides interfaces are present between material layers and may be associated to the kissing bond defect (Oosterkamp et al., (2004)).

3.5. Microhardness profiles

Figure 9 shows the Vickers microhardness (HV) profiles obtained for the four welded specimens, where the values corresponding to measurements obtained in the WN are unfilled, in each case. It can be seen a reduction in hardness from the BM (78 HV) towards the HAZ and WN, for all welding conditions. The advancing side shows a slightly lower HV values, locating in this zone the minimum HV value, for the different D. Considering that the base material has been hardened by cold working, the observed hardness decrease would be associated with the recovery and recristalización in these zones during the welding process. This effect has been reported for strain-hardened alloys (Mishra and Mahoney, 2007).

Furthermore, it can be seen that the hardness in the WN tended to decrease with the shoulder diameter, while the size of the zone where the hardness decreases increased with this parameter. For higher D (D14 and D16) the hardness was the lowest reaching 53-55 HV.

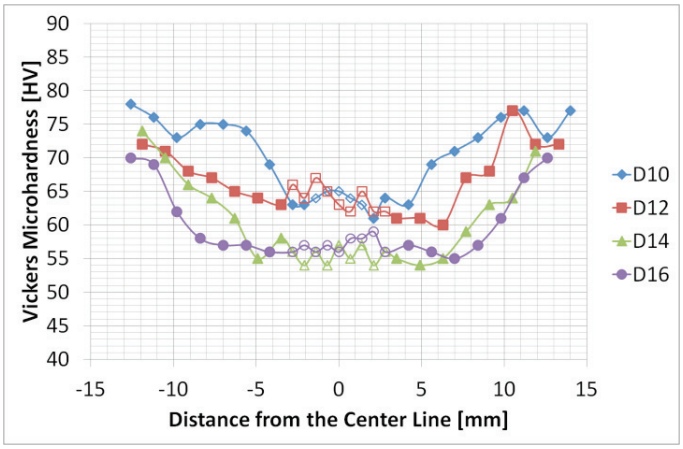

Fig. 9. Vickers microhardness profiles for different tool shoulder diameters.

These phenomena are related to the increase of the thermal field with D, which was previously analyzed and can be represented with PT profiles plotted in Figure 3.a. The higher HI allows achieving the recrystallization temperature in a higher volume of material, associated with the critical strain. Regarding the hardness of the WN, an increase in HI produces an increase in grain size, resulting in hardness decrease.

Finally, it has been observed that the hardness in the HAZ is slightly lower in the advancing side for all hardness profiles. This behavior can be associated with the asymmetry of the FSW process, since it is generally understood that the HI is slightly higher on this side (Nandan et al. (2008)).

4. Conclusions

FSWelds of AA5052-H32 on plates of 3 mm obtained with different tool shoulder diameters were analyzed. Net power values calculated by the FEM model from the acquired thermal cycles increased linearly with the tool shoulder diameter. This increase in power is much less than predicted by the analyzed analytical model for heat generation in FSW, considering that its parameters are constant. This demonstrate the need of introduced the temperature dependence of these parameters. In this way, the linear relationship between these two factors could be explained for both contact conditions (sticking and sliding), considering the decrease in the shear yield stress and the mean pressure with the shoulder diameter.

The effect of the shoulder diameter and the resulting heat generated were related with different characteristics of welded joints. First, the size of the welding nugget increased linearly with power, which is associated with an increase in temperature and plastic flow of material. This plastic flow was lower for the smallest tool shoulder diameter, generating a defect in the base of the welding nugget. There was not observed an effect of shoulder diameter on the zigzag oxide line. The hardness in the welding nugget tended to decrease with shoulder diameter, which would be associated with an increase of grain size. Furthermore, the size of the zone where the hardness decreases increased with the shoulder diameter, which is related to the increase in temperature field.

Therefore, the increasing of the shoulder diameter increased the thermal field and plastic flow, limiting the defects generation and decreasing the hardness. The best balance between these effects was obtained for the shoulder diameter of 12 mm.

Acknowledgements

The authors want to acknowledge to the University of Buenos Aires and INTI for the financial support for this work and to the personnel of the Materials and Structures Laboratory of FIUBA and of the Centre of Mechanics of INTI for its collaboration.

References

Elangovan, K., Balasubramanian, V., 2008. Influences of tool pin profile and tool shoulder diameter on the formation of friction stir processing zone in AA6061 aluminium alloy. Materials and Design 29, 362-373.

Fernández, G., 2009. Soldadura por Fricción Agitación (FSW), Facultad de Ingeniería, Universidad de Buenos Aires.

Mishra, R. S., Ma, Z. Y., 2005. Friction stir welding and processing. Materials Science and Engineering R 50, 1-78.

Mishra, R. S., Mahoney, M. W., 2007. Friction Stir Welding and Processing. ASM Internacional.

Nandan, R., DebRoy, T., Bhadeshia, H. K. D. H., 2008. Recent advances in friction-stir welding - Process, weldment structure and properties. Progress in Materials Science 53, 980-1023.

Oosterkamp, A., Oosterkamp, L. D., Nordeide, A., 2004. 'Kissing Bond' Phenomena in Solid-State Welds of Aluminum Alloys. Welding Journal 83, 225s–231s.

Rajakumar, S., Muralidharan, C., Balasubramanian, V., 2011. Influence of friction stir welding process and tool parameters on strength properties of AA7075-T6 aluminium alloy joints. Materials and Design 32, 535-549.

Schmidt, H. B., Hattel, J. H., 2008. Thermal modelling of friction stir welding. Scripta Materialia 58, 332-337.

Tufaro, L. N., Svoboda, H. G., 2012. Estudio de los Ciclos Térmicos Adquiridos durante FSW mediante Modelos Analíticos y Numéricos. Anais 37th Congresso Nacional de Soldagem, Ouro Preto, Brasil, CT29.